BIOCHEMISTRY
including biophysical chemistry & molecular biology

Article

pubs.acs.org/biochemistry

NMR Studies of DNA Support the Role of Pre-Existing Minor Groove Variations in Nucleosome Indirect Readout

Xiaoqian Xu,[†,‡] Akli Ben Imeddourene,[†,§] Loussiné Zargarian,[†] Nicolas Foloppe,[∥] Olivier Mauffret,*[,†] and Brigitte Hartmann*[,†]

[†]LBPA, UMR 8113, ENS de Cachan CNRS, 61 avenue du Président Wilson, 94235 Cachan cedex, France

[‡]Department of Life Sciences, East China Normal University, 200062 Shanghai, People's Republic of China

[§]Pierre-and-Marie-Curie University, 75005 Paris, France

[∥]51 Natal Road, Cambridge CB1 3NY, United Kingdom

Supporting Information

ABSTRACT: We investigated how the intrinsic sequence-dependent properties probed via the phosphate linkages (BI ↔ BII equilibrium) influence the preferred shape of free DNA, and how this affects the nucleosome formation. First, this exploits NMR solution studies of four B-DNA dodecamers that together cover 39 base pairs of the 5′ half of the sequence 601, of special interest for nucleosome formation. The results validate our previous prediction of a systematic, general sequence effect on the intrinsic backbone BII propensities. NMR provides new evidence that the backbone behavior is intimately coupled to the minor groove width. Second, application of the backbone behavior predictions to the full sequence 601 and other relevant sequences demonstrates that alternation of intrinsic low and high BII propensities, coupled to intrinsic narrow and wide minor grooves, largely coincides with the sinusoidal variations of the DNA minor groove width observed in crystallographic structures of the nucleosome. This correspondence is much poorer with low affinity sequences. Overall, the results indicate that nucleosome formation involves an indirect readout process implicating pre-existing DNA minor groove conformations. It also illustrates how the prediction of the intrinsic structural DNA behavior offers a powerful framework to gain explanatory insight on how proteins read DNA.

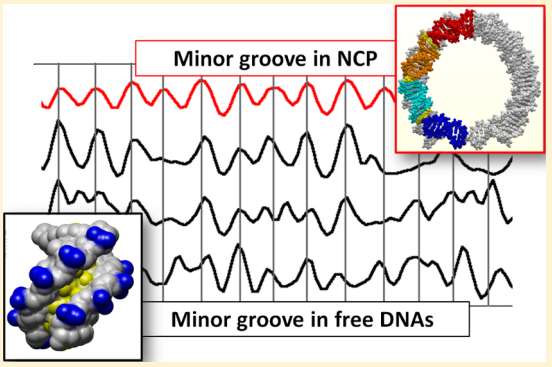

One of the most studied DNA−protein complexes is the nucleosome core particle (NCP), the fundamental building block of packaged DNA in eukaryotic cells. Nucleosomes offer a striking, and yet intriguing, case of indirect readout of DNA by proteins. On one hand, phosphodiester backbone atoms—and not base atoms—are involved in direct or water-mediated DNA−histone contacts.[1−3] Therefore, the NCP formation cannot be guided by direct molecular recognition of the bases. On the other hand, the wrapping of DNA around the histone core requires marked structural DNA deformation, in particular, a bending of 30° per 10 base pairs accompanied by severe groove distortions.[4−6] Thus, the way in which a DNA sequence can intrinsically and specifically modulate the shape and flexibility of the double-helix is thought to be an essential factor in NCP formation.[6−9] Further support for the effect of DNA sequence lies in recurrent lexicographic signatures found in nucleosome positioning sequences.[9−18] In these sequences, two categories of dinucleotides alternate out of phase with a period of ∼10 base pairs (bp): ApA•TpT, TpA•TpA, ApT•ApT on one hand; and GpG•CpC, CpG•CpG, GpC•CpC, CpA•TpG on the other hand. The rationale of such alternations remains poorly understood. For instance, classifications of DNA flexibility inferred from either X-ray DNA structures[19] or stacking energies[18] fall short of accounting for this periodicity. Both approaches categorize the dinucleotides in terms of flexible YpR, intermediate RpR•YpY, and stiff RpY steps whereas each alternating group identified in nucleosomal sequences is composed of a mixture of YpR, RpR•YpY, and RpY.

Several results suggest that, among the 145−147 bp of nucleosomal DNA, particular regions are more critical than others for forming the NCP. The SELEX method has been used to detect artificial DNA sequences with high affinity for the histone core in controlled conditions.[20] The highest-affinity sequence, called sequence 601,[20] is now widely used in biology research for its high ability to position nucleosomes, both *in vitro* and *in vivo*. The alignment of the highest-affinity SELEX sequences[20] has led to the identification of a conserved region covering 73 bp centered around the NCP dyad that illustrate the lexicographic periodicity mentioned above. The importance of this central part of positioning sequences has been further highlighted through analyses of nucleosome occupancy along

Received: April 26, 2014
Revised: August 4, 2014
Published: August 7, 2014

   dx.doi.org/10.1021/bi500504y | *Biochemistry* 2014, 53, 5601−5612

various genomes,[21] and single-molecule experiments on the sequence 601.[22] Interestingly, these findings echo earlier experiments showing that the nucleosome formation is initiated by the deposit of histones H3 and H4,[23,24] which precisely contact the central part of nucleosomal DNA sequences. More specifically, the nucleosome assembly is highly sensitive to the sequence of the two segments located symmetrically at 1.5 double-helix turns from the dyad (SHL ± 1.5, SHL stands for SuperHelix Location).[25] In NCPs crystallized with the human α-satellite sequence,[1,3,8] or sequence 601[26,27] and its derivatives,[5,28,29] SHL ± 1.5 segments are characterized by a spectacular, extremely narrow minor groove; they are implicated in a unique network of interactions involving van der Waals contacts with hydrophobic side chains, Leu65 in H3 and Pro32 in H4, and electrostatic interactions with Arg63 in H3. Sequence 601 contains SHL ± 1.5 elements composed of T•A base pairs that, when they are associated with a marked narrow minor groove, generate a strong electronegative potential which strengthens the interaction with positively charged amino acids.[30] In NCPs, the conjunction of T•A-rich segments and narrow minor groove thus reinforces the interaction with Arg63 at SHL ± 1.5.[31] These observations suggest that T•A-rich sequences associated with pre-existing narrow minor groove could promote the nucleosome formation, strengthening the idea of a role of the sequence-dependent intrinsic DNA properties in indirect readout.

Ideally, identifying structural signatures of DNA sequences that mediate indirect readout during nucleosome formation requires comparison of free, unbound DNA to the same DNA in formed nucleosome. However, practically, deciphering free DNA structural properties in solution remains a challenge.[32,33] That is because free DNA usually deviates only in subtle ways from a regular B-double helix, and this small deviations are difficult to ascertain experimentally or computationally.

Recently, the modulation of the structure of free B-DNA has been characterized in solution by considering the phosphate group BI↔BII equilibrium, which is sequence-dependent and closely related to the overall shape of B-DNA.[33,34] In B-DNA in solution, the phosphate groups oscillate between two states, defined by the torsion angles ε and ζ, *trans*/*g*- in BI (ε–$\zeta \sim -90°$) and *g*-/*trans* in BII (ε–$\zeta \sim +90°$) (Figure 1).[35,36] This conformational transition occurs on a nanosecond time scale.[37] The BII propensity of each phosphate can be determined in solution by NMR, from the ^{31}P chemical shifts (δP).[38,39] Importantly, each of the 16 B-DNA dinucleotides is characterized by a specific δP value.[34] Hence, specific BII propensity scores were proposed to describe and predict the backbone behavior at the dinucleotide level.[34]

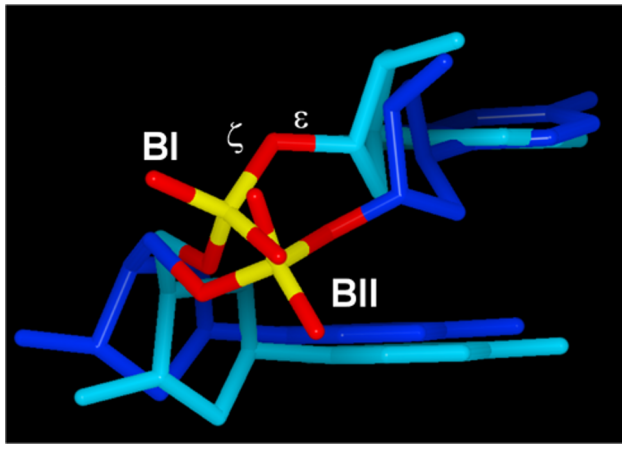

Figure 1. BI and BII conformations. Illustration of the BI (bases and sugars in light blue, (ε–ζ) = −90°) and BII (bases and sugars in dark blue, (ε–ζ) = +90°) phosphate linkage conformations with a CpC dinucleotide.

In addition, analyses of X-ray structures and molecular modeling studies showed that the conformations of the phosphates of a complementary dinucleotide, BI•BI, BI•BII (and its counterpart BII•BI) or BII•BII, are associated with distinctive values of the local, inter-base-pair parameters of twist, roll, and slide.[38,40−45] A recent modeling study mentioned that rise, tilt, and shift are also affected by the backbone states.[46] Twist, roll, and slide are the major factors associated with B-DNA structure variability.[19] Dinucleotides in BI are associated with low twist, null, or positive roll, and negative slide (BI profile). Dinucleotides in BII are characterized by high twist, negative roll, and positive slide (BII profile). Some dinucleotides are essentially confined to the BI state and the associated local helicoidal BI profile. In contrast, dinucleotides with a significant BII population explore a larger conformational landscape corresponding to both BI and BII profiles.

In B-DNA X-ray structures, the groove shape within tetramer segments is also related to the BII density, via a cumulative effect on base-pair displacement (X-disp).[47−49] BI-rich tetramers present a typical narrow minor groove, while an accumulation of BII phosphate groups favors a more open and accessible minor groove (Figure 2).[47,48] This intrinsic DNA property is exploited by minor groove binding proteins.[47,50] Thus, the BI and BII states correlate with the sequence-dependent intrinsic DNA variability in structure, which in turn influences the molecular recognition of DNA via indirect readout.

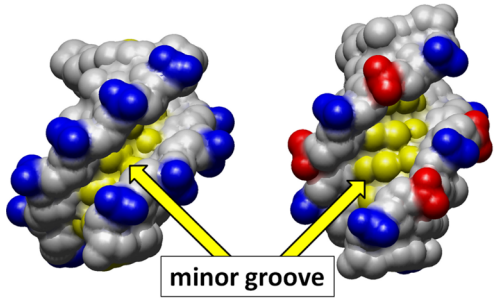

Figure 2. Illustration of the structural relationship between BI- or BII-rich regions and the DNA minor groove width. The GpG•CpC dinucleotides contain two facing phosphate groups either in BI (left, BI phosphate groups in blue) or in BII (right, BII phosphate groups in red). The yellow arrows emphasize the minor grooves, either narrow (left) or wider (right). The base atoms constituting the minor groove floor are in yellow. The structures were extracted from DNA crystal structures with PDB entries 1EHV and 3GGI.

In sum, δPs and BII propensities are useful and convenient surrogate reporters to inform about the DNA shape and its sequence dependent variation in solution. In reference to the relationship observed in X-ray structures between BI/BII states, Twist, Roll, and X-disp, the so-called TRX scale was proposed to characterize the 10 complementary dinucleotides by their BII propensities, inferred from a large data set of δPs.[34]

On the basis of the above findings, we investigate here how the intrinsic DNA properties influence the sequence-dependent formation of the NCP. We used NMR to study four constituent

dx.doi.org/10.1021/bi500504y | *Biochemistry* 2014, 53, 5601−5612

overlapping dodecamers of the sequence 601. Together, these oligomers cover a nonoverlapping 39 bp segment in the 5′ half of sequence 601 (from −4 to −0.1 in terms of SHL) (Figure 3). Oligomer 3 is centered on the TTAAA element situated at SHL ± 1.5 in the NCP, which is potentially a stringent singular positioning signal, as explained above.

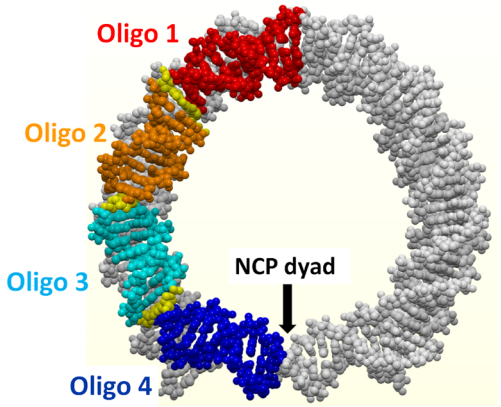

Figure 3. Location of the four studied dodecamers in Nucleosome Core Particle (NCP). Four dodecamers overlapping by three bases (Oligo 1−4, sequences given in Table 1) were studied in their free (unbound) state by NMR. The juxtaposition of the four oligomers recomposes a sequence that corresponds to part of the 5′ half of the DNA sequence 601 (from −4 to −0.1 in terms of SHL). Here, the four dodecamers are positioned on the structure of the sequence 601 within NCP (PDB entry 3MVD) in which the DNA is wrapped twice around the histone core (not shown in this figure). Oligo 1 is in red, Oligo 2 in orange, Oligo 3 in light blue, and Oligo 4 in dark blue. The base pairs in yellow correspond to the overlapping bases in the free studied dodecamers.

We start the present study with methodological elements. First, examination of the temperature-dependence of ^{31}P chemical shifts enabled us to further validate the method relating BII percentages to ^{31}P chemical shifts.[38] Second, the new BII percentages inferred from the ^{31}P chemical shifts measured for the four oligomers provided a stringent test for the previously proposed prediction of BII scores from DNA sequence.[34] The predicted BII propensities were found in excellent agreement with the new BII percentages gathered on the four oligomers, proving that the BII propensities can be predicted from sequence alone. Third, the NMR data also confirmed that BII density is coupled to minor groove width as previously inferred from X-ray structure analysis.[47]

We then investigated the relationship between minor groove width variations in the NCP and their counterparts in free DNA, which are represented by backbone intrinsic BII propensity. One of the most interesting features of DNA in the nucleosome is the periodic ("sinusoidal") alternation of wide and narrow minor grooves, located outward and inward from the histone core, respectively.[4−6] The location of minor groove width minima and maxima is remarkably maintained over 35 X-ray nucleosome structures,[6] while the distribution of slide and roll are quite variable along the DNA sequences.[4] By extending the prediction of intrinsic BII propensities to the whole sequence 601 and five other artificial sequences of high or low affinity for the histone core, the present work uncovers a parallel between the intrinsic properties of DNA free in solution and the distortions of DNA observed in X-ray structures of the NCPs. This provides new insights into the ability of sequences at forming NCPs, and suggests an indirect readout of the DNA groove shape.

MATERIALS AND METHODS

DNA Sequences. Four oligodeoxyribonucleotides of 12 base pairs (bp) were studied by NMR. Their sequences are given in Table 1. The sequences of these dodecamers overlap by three bases. These overlaps make it possible to splice the four oligomers without considering the terminal base pairs, subject to end effects. For instance, Oligo 1 ends with $G_{10}C_{11}T_{12}$ and Oligo 2 begins with the same motif, $G_1C_2T_3$. The NMR data of the terminal dinucleotides $C_{11}T_{12}$ and G_1C_2 were discarded for the analyses while those collected for the penultimate $G_{10}C_{11}$ and C_2T_3 steps were considered.

The four juxtaposed dodecamers recompose a 39 bp sequence (Table 1) that corresponds to part of the non-palindromic sequence 601 of 146 bp (Table 1). The sequence 601 was selected for its very high-affinity for association with the histone octamer, as detected in SELEX experiments.[20] The center of the sequence 601 defines two 73 bp halves. In NCP structures, this DNA center corresponds to the pseudo-twofold axis of symmetry, the NCP dyad. According to the conventions suggested for the description of the first X-ray structure of NCP,[3] the rotational orientation of the DNA is defined relative to the DNA center (SuperHelix Location zero, or SHL0). For each successive turn, the location number increases in the 3′ half up to SHL+7, and decreases in the 5′ half down to SHL-7. The four dodecamers studied by NMR corresponds to the segment from SHL-4 to SHL-0.1 in NCP (Figure 3).

Sample Preparation. Oligomers were synthesized by Eurogentec Inc. (Belgium). The sample was dissolved in an aqueous sodium phosphate buffer corresponding to an ionic strength of 0.1 (mol/L) with 0.1 mM EDTA, at pH 6.5. The duplexes were prepared by mixing the two complementary strands in a 1:1 ratio in 450 μL H_2O and 50 μL D_2O for studies

Table 1. Sequences of the Four Contiguous DNA Dodecamers Constituents of the Sequence 601[a]

Oligo 1	5′-TCGTAGCAAGCT-3′•5′-AGCTTGCTACGA-3′
Oligo 2	5′-GCTCTAGCACCG-3′•5′-CGGTGCTAGAGC-3′
Oligo 3	5′-CCGCTTAAACGC-3′•5′-GCGTTTAAGCGG-3′
Oligo 4	5′-CGCACGTACGCG-3′•5′-CGCGTACGTGCG-3′
39 bp	$T_1C_2G_3T_4A_5G_6C_7A_8A_9G_{10}C_{11}T_{12}C_{13}T_{14}A_{15}G_{16}C_{17}A_{18}C_{19}C_{20}G_{21}C_{22}T_{23}T_{24}A_{25}A_{26}A_{27}C_{28}G_{29}C_{30}A_{31}C_{32}G_{33}T_{34}A_{35}C_{36}G_{37}C_{38}G_{39}$
Sequence 601	TGGAGAATCCCGGTGCTAAGGCCGCTCAATTGGTCGTAGCAAGCTCTAGCACCGCTTAAACGCACGTACGCGC‖TGTCCCCCGCGTTT-TAACCGCCAAGGGGATTACTCCCTAGTCTCCAGGCACGTGTCAGATATATACATCCTGT

[a]Four oligomers were studied free in solution by NMR. Their sequences overlap end to end by three bases (underlined). These overlaps make it possible to juxtapose the central parts of the four oligomers without considering the terminal base pairs (subject to end effects) and to recompose a continuous 39 bp sequence corresponding to part of the sequence 601. The 5′ → 3′ sequence of this 39 bp segment and its numbering are shown below the sequences of the oligomers. The last row corresponds to the 5′ → 3′ sequence 601 of 146 bp; its center, indicated by a double bar, defines two 73 bp halves of a same strand; the 39 bp fragment is underlined (see also Figure 3).

dx.doi.org/10.1021/bi500504y | Biochemistry 2014, 53, 5601−5612

Table 2. Predicted BII Percentages of Complementary Dinucleotides in B-DNA[a]

		sequence	BII_{i_av}%•BII_{j_av}%	BII_{i,j_av}%	SD BII_{i,j_av}%
complementary dinucleotides	YpR•YpR	CpG•CpG	43•43	43	16
		CpA•TpG	52•31	42	18
		TpA•TpA	14•14	14	7
	RpR•YpY	GpG•CpC	47•37	42	11
		GpA•TpC	33•11	22	15
		ApG•CpT	18•0	9	15
		ApA•TpT	11•0	5	12
	RpY•RpY	GpC•GpC	25•25	25	11
		ApC•GpT	8•0	4	13
		ApT•ApT	0•0	0	14
3′- and 5′-neighbor effect	CpG•CpG	YCpGR•YCpGR	59•59	59	19
		YCpGY•RCpGR	51•51	51	14
		RCpGY•RCpGY	38•38	38	17
	CpA•TpG	YCpAR•YTpGR	77•42	59	8
		YCpAY•RTpGR	59•21	40	11
		RCpAR•YTpGY	33•28	30	18
		RCpAY•RTpGY	36•19	27	17

[a]The 10 complementary dinucleotides $Np_iN•Np_jN$ are characterized by BII_{i,j_av}%, which are the half-sums of the individual BII_{i_av}% and BII_{j_av}% of two facing phosphates. These BII percentages were previously extracted from a data set of 323 δP.[34] The BII percentages of CpG•CpG and CpA•TpG are also given considering the effect of their 3′- and 5′-nearest neighbors, expressed in terms of purine (R) and pyrimidine (Y). The standard deviations (SD) given for BII_{i,j_av}% were inferred from the δP variabilities (see Materials and Methods).

of exchangeable protons. For studies of nonexchangeable protons, the duplexes were lyophilized three times and dissolved in 500 μL of 99.9% D_2O. The final concentration of double strand oligomers is 1−1.5 mM.

NMR Spectroscopy. All NMR spectra were recorded on a Bruker Avance spectrometer operating at a proton frequency of 500 MHz and at a phosphorus frequency of 202 MHz with a 5 mm gradient indirect probe. All spectra were processed with NMRpipe[51] and analyzed with Sparky (T. D. Goddard and D. G. Kneller, SPARKY 3, University of California, San Francisco).

One-dimensional ^{1}H spectra collected from 5 to 60 °C with a 5 °C step enabled us to check that the duplexes were stable over this range of temperatures. All the imino protons were clearly observable at 50 °C, except those of the terminal base pairs.

^{1}H NMR studies were performed at 10, 20, and 30 °C. 2D NOESY spectra were recorded using mixing times of 100, 200, and 300 ms for exchangeable protons and 80, 100, 200, 300, and 400 ms for nonexchangeable protons. MLEV-17 TOCSY experiments were run using mixing time of 120 ms. The 2D NOESY and MLEV-17 TOCSY were recorded under the following experimental conditions: 2048 data points and 512 t1 increments with spectral widths of 10 000 Hz for exchangeable protons and 5000 Hz for nonexchangeable protons. The water signal was suppressed with a WATERGATE sequence.[52] NOE distances were extracted from cross-peaks with particular care after visual inspection of the build-up rates and using the distance extrapolation method to correct the spin-diffusion effects.[53] Distances were normalized using the cytosine H5−H6 proton pairs (r = 2.5 Å) apart from those involving the CH_3 group, for which the reference was the average H6−CH_3 distance (r = 2.9 Å). The experimental error on distances is estimated to 10% of the measured distances.

^{1}H−^{31}P HETCOR[54] experiments were run at 20, 30, and 40 °C. The spectra width was 2500 Hz in the ^{1}H dimension and 810 Hz in the ^{31}P dimension. Data were recorded with 2048 points in the ^{1}H dimension and 256 increments in the ^{31}P dimension. ^{31}P chemical shifts were referenced relative to internal trimethyl phosphate. Uncertainty of ^{31}P chemical shift measured in solution is estimated to ±0.02 ppm.

Apart from the section ^{31}P Chemical Shifts to Characterize the DNA Backbone Behavior", the NMR data presented here were collected at 20 °C.

All the NMR data are available in the Biological Magnetic Resonance Bank (BMRB) entry 19222.

BII Propensities. BII percentages (BII%) of the phosphate linkages along the four dodecamers were inferred from the δPs measured here at 20 °C using the equation BII(%) = 143 δP + 621 (δP referenced to trimethyl phosphate).[38] BII% were used in the section ^{31}P Chemical Shifts to Characterize the DNA Backbone Behavior.

In the section Validation of the DNA Sequence Effect on the Backbone Behavior with the Dodecamers, we considered the BII propensity of the complementary dinucleotides $Np_iN•Np_jN$ defined as the half-sum of the individual BII percentages of the facing phosphates p_i and p_j: $BII_{i,j}$% = (BII_i% + BII_j%)/2. In Table 2, the 10 complementary dinucleotides $Np_iN•Np_jN$ are characterized by specific $BII_{i,j}$% previously published.[34] The corresponding standard deviations were inferred from the δP variabilities between various instances of a given step, which are on average ±0.10 ppm. These variances dominate the δP experimental errors (±0.02 ppm) that were therefore neglected.

In Relation between BII Propensities and Minor Groove Width Validated in Solution with NMR and Implications for the Preferential Interaction of DNA Sequences with the Histone Core, we defined an extended BII score, $BII_{i,j\ ext}$%, in order to take into account the effect of the 5′ and 3′ neighbors on the base pair displacements of $Np_iN•Np_jN$, which are related to groove dimensions.[47] Thus, the complementary dinucleotides $Np_iN•Np_jN$ are characterized by $BII_{i,j\ ext}$%, the averaged sum of the individual $BII_{i,j}$% of the three complementary dinucleotides in the tetramer $Np_{i-1}Np_iNp_{i+1}N•Np_{j-1}Np_jNp_{j+1}N$: $BII_{i,j\ ext}$% = ($BII_{i-1,j+1}$% + $BII_{i,j}$% + $BII_{i+1,j-1}$%)/3.

Crystallographic NCP Structures. In the context of this study, we examined the three NCP structures crystallized with sequence 601 of either 145 bp (PDB entries 3ZL0 and 3ZL1,

dx.doi.org/10.1021/bi500504y | Biochemistry 2014, 53, 5601−5612

resolution of 2.5 Å[27]) or 146 bp (PDB entries 3MVD, resolution of 2.9 Å[26]). The additional base in 3MVD is located at the end of the sequence (...CGAT-3′ instead of···GAT-3′ in 3LZ0 and 3LZ1). The 3MVD structure contains the chromosome condensation regulator RCC1 that contacts three phosphate groups without disturbing the overall DNA structure, according to our analyses. Analyses of NCP structures were carried out using Curves+.[55]

Graphics. Graphical representations were prepared with Yasara (http://www.yasara.org/).

RESULTS AND DISCUSSION

^{31}P Chemical Shifts to Characterize the DNA Backbone Behavior. The ^{31}P chemical shift (δP) values reflect the two-state BI ↔ BII equilibrium (Figure 1). High- and downfield shifted δPs correspond to BI- and BII-rich phosphate groups, respectively.[36,37] The four oligomers studied here (Table 1) correspond to 72 dinucleotide steps, excluding the terminal steps. All 72 δPs were assigned and measured at 20, 30, and 40 °C (Table S1 in Supporting Information). They cover a range typical of B-DNA, from −3.80 to −4.51 ppm. Examples of ^{1}H−^{31}P HETCOR spectra are shown in Figure 4.

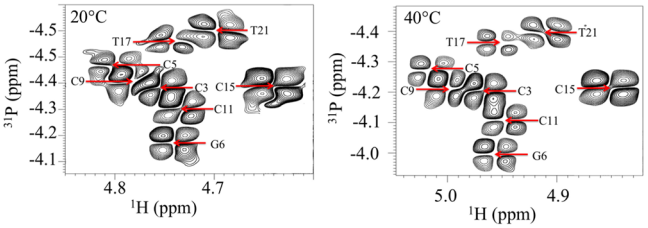

Figure 4. Representative ^{1}H−^{31}P HETCOR spectra for δP determination. The ^{1}H−^{31}P HETCOR spectra show a section of the H3′-P region obtained for Oligo 4 at 20 °C (left panel) and 40 °C (right panel). The red arrows indicate the cross-peak centers.

Two empirical relations were proposed to translate δPs in terms of BII percentages,[38,39] using eq 1[38] or 2 at 20 °C.[39]

$$\text{BII\%} = 143\delta\text{P} + 621 \quad (1)$$

$$\text{BII\%} = 114.84\delta\text{P} + 515.62 \quad (2)$$

These equations were obtained with two different methods, which both assume implicitly[38] or explicitly[39] that δP of pure BI and pure BII states are sequence-independent. This assumption is very difficult to test by NMR, since, to our knowledge, no other experimental method can identify which dinucleotide would be strictly confined in only one state. A recent interesting computational study, combining molecular dynamics simulations on the Drew-Dickerson dodecamer and quantum mechanical calculations of δP, suggested that the backbone angle values are sensitive to the dinucleotide sequence; according to DFT calculations on DNA fragments, these sequence dependent variations would affect the δP values of pure BI and BII states.[56] Although eqs 1 and 2 do not yet integrate such refinement, the overall consistency of the results presented below indicates that they are robust for estimating BII%.

Examining the behavior of the phosphate linkages as a function of temperature enabled to estimate the δP value that does not vary with temperature. This particular value is expected to be the signature of equal populations of BI and BII (BII% = 50).[57,58] The temperature study investigated the influence of a moderate increase of temperature on the BI ↔ BII equilibrium by collecting δPs at 20, 30, and 40 °C, on integrally preserved double helices. The δP values changed by 0.043 ± 0.022 ppm on average between 20 and 40 °C (typical changes in Figure S1 in Supporting Information). Such slight but significant variations of the same magnitude were previously observed on other oligomers.[39,58]

The variation of δP between 20 and 40 °C ($\Delta\delta$P) is negatively correlated to the reference δP values at 20 °C (Figure 5).

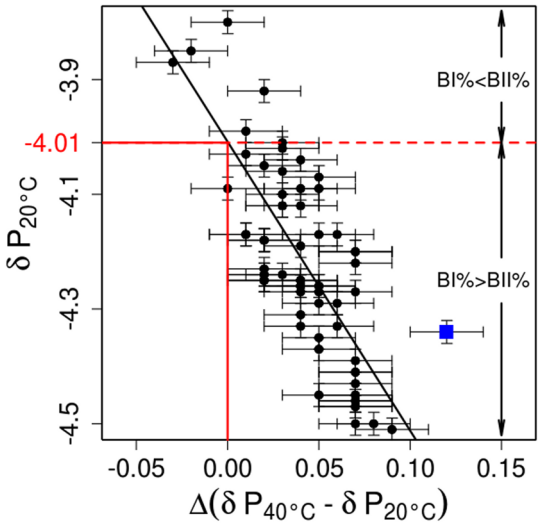

Figure 5. Relationship between the amplitude of ^{31}P chemical shift changes according to temperature and the down- or high-field character of phosphate linkages. The ^{31}P chemical shift change between 20 and 40 °C ($\Delta(\delta P_{40°}-\delta P_{20°})$, ppm) is linearly correlated to δP measured at 20 °C ($\delta P_{20°}$, ppm). The phosphate linkage of ApA (blue square) in the TTAA segment of Oligo 3 has an unusual behavior (see the text). The black line corresponds to the linear fit of the data, discarding δP of ApA in TTAA. $\Delta(\delta P_{40°}-\delta P_{20°}) = 0$ (marked in red) theoretically corresponds to a BI/BII ratio of 1. Accordingly, $\delta P_{BI/BII=1} = -4.01$ ppm. $\delta P > \delta P_{BI/BII=1}$ and $\delta P < \delta P_{BI/BII=1}$ correspond to a majority of BII and BI conformers, respectively. The bars are the experimental errors.

Positive and negative $\Delta\delta$Ps correspond to increasing and decreasing BII populations, respectively. The most marked variations are the positive $\Delta\delta$Ps observed on steps with high or very high BI population at 20 °C (δPs typically between −4.5 and −4.2 ppm; see Figure 5). This behavior was observed before, above 20° for BI-rich steps.[58] Although a full understanding of this observation will ultimately require a detailed analysis, our results show that BI-rich steps gain some BII character under external stress—here, the temperature increase. Yet, one BI-rich step, A_7pA_8 in Oligo 3, shows an exceptional $\Delta\delta$P of +0.12 ppm (Figure 5 and Figure S1 in Supporting Information). The examination of 1D ^{1}H spectra led to the detection of slight H2 and H8 resonance broadenings on A_7 and A_8, which may indicate transient excursions toward unknown low-populated conformations requiring sophisticated NMR experiments to be confirmed.[59] For this reason, the $\Delta\delta$P corresponding to A7pA8 was discarded from the analysis.

The linear fit of the correlation between δP20° and $\Delta\delta$Ps is characterized by a correlation coefficient of 0.76 and a standard deviation of 0.10 ppm. This fit enables to estimate that $\Delta\delta$P = 0 (the point for which no change in δP occurs with temperature variation) corresponds to a δP value of −4.01 ± 0.10 ppm at 20 °C (Figure 5). Interestingly, this δP value is very similar to the average δP value previously found for random coil DNAs,

dx.doi.org/10.1021/bi500504y | Biochemistry 2014, 53, 5601−5612

which is centered around 4.0 ppm, with a sequence dependent range of ±0.2 ppm.[57] According to eqs 1 and 2, a δP value of −4.01 ± 0.10 ppm corresponds to BII% = 48 ± 7 (eq 1) or BII% = 55 ± 6 (eq 2). Thus, both eqs 1 and 2 predicted reasonable BII%, compatible with what is expected for $\Delta\delta P = 0$, i.e., equal populations of BI and BII. This indicates that neglecting a possible sequence effect on δPs of pure BI and pure BII is tenable in practice.

Since the data are not sufficient to discriminate between eqs 1 and 2, in the remainder of the present study, eq 1[38] was used to convert to BII percentages the δPs collected at 20 °C.

The average BII percentages ($BII\%_{av}$) were calculated from the average δPs (δP_{av}), themselves deduced from the 72 δPs collected on the four dodecamers at 20, 30, and 40 °C. $BII\%_{av}$ are 16.2 (δP_{av} = −4.23 ppm) at 20°, 19.4 (δP_{av} = −4.20 ppm) at 30 °C, and 22.2 (δP_{av} = −4.19 ppm) at 40 °C. These values are broadly consistent with the ∼20% of BII conformers inferred from statistics from X-ray structures[40] or from δP in solution,[34,38] without considering the temperature. Superficially, that would initially suggest that there is no distinctive pattern regarding the BI−BII character in sequence 601. Yet, the BII percentages vary considerably along the dodecamer sequences and some phosphate groups exhibit 40% or more of BII conformers (Figure 6). These variations hide a strong sequence effect, which is addressed below.

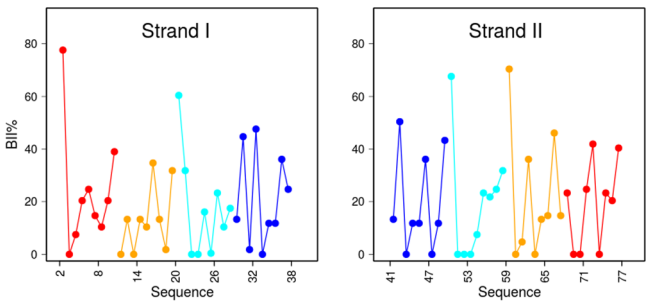

Figure 6. Experimental BII percentages along the four dodecamers. The BII percentages (BII%) were inferred from the ^{31}P chemical shifts at 20 °C and plotted along the two strands of the oligomers, shown in order from end to end (numbering of strand I detailed in Table 1). The terminal dinucleotides, subject to end effects, were not considered. Oligo 1 is in red, Oligo 2 in orange, Oligo 3 in cyan, and Oligo 4 in blue. The left and right panels correspond to the first and the second 5′ → 3′ strands, respectively.

Validation of the DNA Sequence Effect on the Backbone Behavior with the Dodecamers. Here, we consider the complementary dinucleotides, $Np_iN{\bullet}Np_jN$, rather than the dinucleotides isolated from their partner. This approach is justified since the B-DNA mechanics imparts a strong coupling between the conformational states of two facing phosphate linkages, BI•BI, BI•BII, and BII•BII; in turn, these combinations of facing backbone states are coupled to the inter base pair parameters of slide, roll, and twist.[38,40−46] X-ray structure analysis showed that the facing backbone combinations delineate zones in the roll/twist space with negligible overlaps.[32,40,41] In DNA studied by modeling, BII•BII are rare, but helical parameter values, especially for the twist, can be decomposed into Gaussian-like distributions corresponding to the BI•BI and BI•BII states.[46] Considering the double helix structure, it is thus more relevant to consider the BII propensities of two facing phosphates than those of each phosphate separately. In addition, two facing phosphates tend to behave similarly.[34] This property is retrieved with the data collected here, the difference between the BII percentages of two facing phosphates being on average 15%. Hence, each $Np_iN{\bullet}Np_jN$ is characterized by the half-sum of the BII percentages of its facing phosphates i and j ($BII_{i,j}\% = (BII_i\% + BII_j\%)/2$).

It has emerged that the BI↔BII equilibrium primarily depends on the dinucleotide sequence.[34,38,40] From an extensive δP data set, the 10 complementary dinucleotides composing B-DNA were characterized each by specific $BII_{i,j}\%_i$ values, presented as the TRX scale.[34] For convenience, these values are reported in Table 2, introducing explicitly the effect of the 3′- and 5′-nearest neighbors on CpG•CpG and CpA•TpG. These two steps are particularly sensitive to their nearest neighbors, 5′-Y/3′-R and 5′-R/3′-Y neighbors increasing and decreasing the BII populations, respectively.[38,60,61] As this previous study[34] proposed that BII propensities can be deduced from the sequence, Table 2 and the underpinning training set of data may be seen as providing predictions which may be tested with subsequently obtained $BII_{i,j}$ values.

The four dodecamers contain six complementary dinucleotides present in several copies—6 ApC•GpT, ApG•CpT and GpC•GpC, 5 CpG•CpG and 4 ApA•TpT and TpA•TpA—which enabled confirmation that each of these complementary dinucleotide types is characterized by an average $BII_{i,j}\%$ value (Figure S2 in Supporting Information). More extensively, $BII_{i,j}\%$ calculated from all the new δPs measured here on the dodecamers were compared with their predicted counterparts from Table 2. These two quantities coincide for all the dinucleotides composing the four dodecamers (Figure 7). Actually, taking into account the effect of the tetrameric environment on CpG•CpG and CpA•TpG enabled us to obtain a remarkable fit between the profiles of newly determined and predicted $BII_{i,j}$ propensities along the four dodecamers (Figure 7). So, the δPs measured here on the dodecamers confirmed and reinforced the previous findings on B-DNA sequence-dependent intrinsic backbone behavior. It essentially demonstrates that the BI−BII character of phosphate linkages in B-DNA free in solution is predictable from the sequence. Thus, it provides a strong ground to investigate how the distribution of the dinucleotides with low and high BII propensities is relevant along any DNA sequence owing to the coupling with DNA shape, which is now examined.

Relation between BII Propensities and Minor Groove Width Validated in Solution with NMR. DNA groove widths are measured between two residues on opposite strands, which are closest in space across the groove. These residues are staggered by two or three nucleotides in the 3′ direction.[62] In free DNAs, the groove dimension measured on $Np_iN{\bullet}Np_jN$ is related to the conformational states of the phosphate groups of the central dinucleotide of interest and of its 3′- and 5′-neighbors, i.e., $Np_{i-1}Np_iNp_{i+1}N{\bullet}Np_{j-1}Np_jNp_{j+1}N$, mainly because of the cumulative effect of the backbone conformational states on base-pair displacement.[47] In other words, BI or BII density within a 4 bp segment is coupled to the groove dimensions.[47] This led to characterization of $Np_iN{\bullet}Np_jN$ by an extended BII score, BII_{i,j_ext}, which takes into account the neighbors of $Np_iN{\bullet}Np_jN$, by averaging the individual $BII_{i,j}$ percentages of the three complementary dinucleotides in $Np_{i-1}Np_iNp_{i+1}N{\bullet}Np_{j-1}Np_jNp_{j+1}N$ ($BII_{i,j\ ext}\% = (BII_{i-1,j+1}\% + BII_{i,j}\% + BII_{i+1,j-1}\%)/3$; see also Materials and Methods).[47] A main finding of this previous study[47] concerned the minor groove width. Classical narrow minor grooves are associated

dx.doi.org/10.1021/bi500504y | Biochemistry 2014, 53, 5601−5612

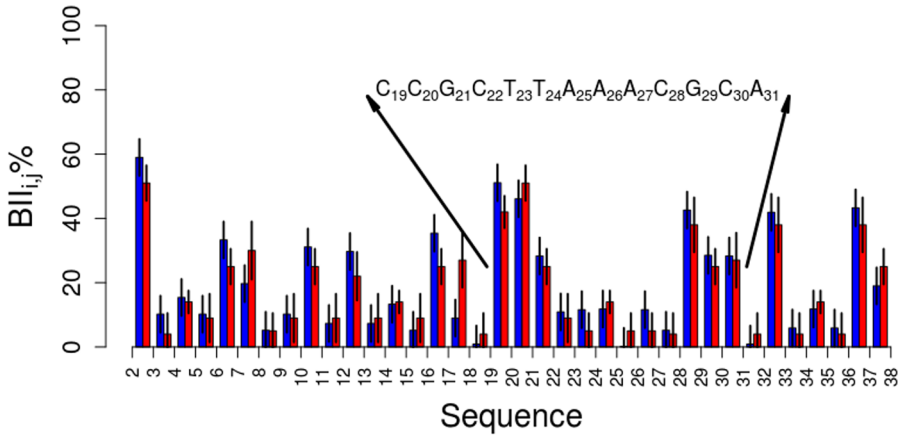

Figure 7. Sequence effect on BII propensities of the complementary dinucleotides forming a part of the 5′ half of sequence 601. The complementary dinucleotides are characterized by the half-sum of the BII percentages of their facing phosphates: $BII_{i,j}\% = (BII_i\% + BII_j\%)/2$. These quantities are either inferred from the experimental δP values measured in this study (blue bars) or predicted (red bars) from the analysis of an extensive δP data set previously published (Table 2[34]). The small vertical black bars are the errors, either calculated from the experimental errors on δPs measured in this study for the corresponding $BII_{i,j}\%$ or from the standard deviations for predicted $BII_{i,j}\%$. The sequence explicitly given is centered on the T:A rich segment located at a 1.5 double-helix turn from the dyad (SHL-1.5) in the NCP. The sequence and the numbering are detailed in Table 1.

with low BII density tetramers (low BII_{i,j_ext} values) whereas enlarged minor grooves correspond to segments with high BII density (high BII_{i,j_ext} values),[47] as illustrated in Figure 2.

In NMR, the minor groove width can be investigated on A•T base pairs through the NOE resonances between the H2 of adenine and the H1′ located across the strand (Scheme 1),

Scheme 1. H2−H1′ Inter-Strand Distances (Å) in Oligos 1, 3, and 4[a]

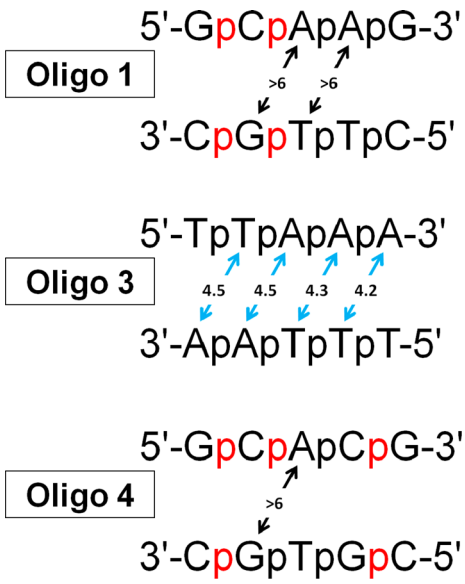

[a]The BI- and BII-rich phosphate linkages are in black and red, respectively. Black arrows indicate the distances potentially observable in the NMR spectra, but not actually discernible. Blue arrows correspond to measured distances.

which are detectable only in the case of narrow minor groove.[63] The NMR data collected here along the free BI-rich TTAAA region of Oligo 3 show observable and measurable H2−H1′ interstrand distances in spectra recorded with 100, 200, and 400 ms (Scheme 1, Figure 8). In addition, Oligo 1 and 4 contain adenines that provide interesting information about the minor groove width in BII-rich segments. Even using a long mixing

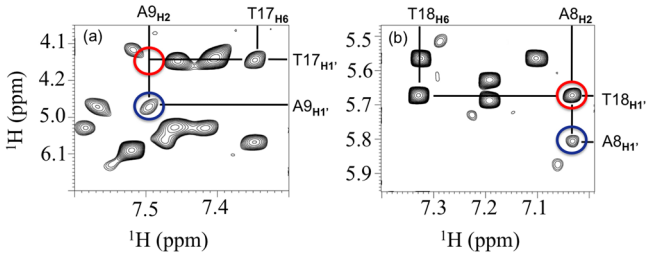

Figure 8. Representative ^{1}H−^{1}H NOESY spectra of H2−H1′ interstrand connectivities. The NOESY spectra show a section of the Base-H1′ region obtained for Oligo 1 (left panel) (a) and 3 (right panel) (b) at 20 °C, using a mixing time of 400 ms. In Oligo 1 (left panel) (a), no connectivity is detected between H2 of A9 in strand 1 and H1′ of T17 in strand 2. Its theoretical location is indicated by a red circle. By comparison, the intrastrand connectivity observed between H2 and H1′ of A9 appears very clearly (blue circle). In Oligo 3 (right panel) (b), the interstrand connectivity observed between H2 of A8 in strand 1 and H1′ of T18 in strand 2 (red circle) is stronger than the intrastrand connectivity between H2 and H1′ of A8 (blue circle). Such marked cross-peaks also exist for the couples T6-A19, A7-T18, and A9-T16 in Oligo 3. The four interstrand H2−H1′ connectivities in Oligo 3 were observed from a mixing time of 100 ms.

time of 400 ms, the H2−H1′ interstrand cross-peaks of adenines in or near CpA steps are missing while they could be theoretically observed in the ^{1}H−^{1}H spectra (Scheme 1, Figure 8). The corresponding distances are thus larger than 6 Å, beyond the limit of NMR detection.

Our measurements thus provide clear evidence that sustained narrow minor grooves exist in free TTAAA elements in solution. They emphasize that a region composed of a succession of BI-rich steps in solution (such as TTAAA) corresponds to a narrow minor groove shape, while BII-rich regions correspond to a wider minor groove. This result validates in solution the relation between BII density and groove shape previously reported on the basis of X-ray structures.[47]

Implications for the Preferential Interaction of DNA Sequences with the Histone Core. We now analyze how the intrinsic structural preferences of free sequences may be relevant for forming the NCP. We focus on the minor groove width because its variation is the most remarkable, recurrent characteristics

dx.doi.org/10.1021/bi500504y | *Biochemistry* 2014, 53, 5601−5612

of DNA across NCP X-ray structures, regardless of the DNA sequence.[4−6] This feature is further highlighted by our analysis showing that the correlation coefficient between the minor groove width values calculated on NCPs crystallized with the human α-satellite on one hand and the sequence 601 on the other hand is 0.75. By comparison, the correlation coefficients calculated on the same structures but for roll and slide values are clearly lower, 0.47 and 0.27, respectively. This suggests that the histone core imposes a unique pattern of minor groove variation to DNA upon binding. In NCPs, these conserved wide and narrow minor grooves, which alternate with a periodicity of approximately 10 bp (Figure 9), are located outward and inward from the histone core, respectively.

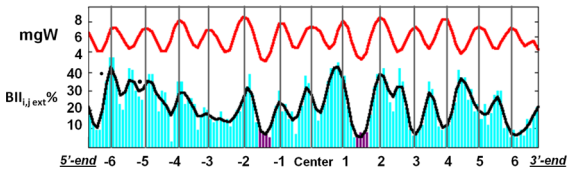

Figure 9. Intrinsic extended BII propensities of the free sequence 601, compared to variation of the minor groove width in the NCP. The intrinsic backbone behavior is expressed in terms of BII$_{i,j\ ext}$% (see the text and Materials and Methods) predicted for each complementary dinucleotide composing the sequence 601, and represented as bars. BII$_{i,j\ ext}$% for the TTAAA elements are in violet, all the others in cyan. Variations in BII$_{i,j\ ext}$% along the sequence are traced with a black line (using a natural smoothing spline approximation to the bars). The sinusoidal variations of the minor groove width (mgW, Å) in the NCP are shown at the top of the panel (red line). These values were calculated and averaged on the NCP X-ray structures containing sequence 601 (PDB entries 3LZ0, 3LZ1, and 3MDV). The vertical gray lines mark the maximal values of minor groove width, expressed in terms of SHL, starting from the center of the sequence 601 ("Center", at position 73.5 in the 146 bp sequence 601). Apart from the end of the 3′ part of sequence 601 (SHL > +2.5), the minor groove distortions in NCP follow the intrinsic extended BII propensities, in turn coupled to groove dimensions in free DNA.

As stated in the previous sections, intrinsic BII propensities can be predicted rather safely from Table 2. The extended BII scores, BII$_{i,j\ ext}$%, calculated from the BII% of the dodecamers, match very well their predicted counterparts (Figure S3 in Supporting Information, correlation coefficient of 0.9). BII$_{i,j\ ext}$% prediction was first applied to the whole sequence 601 and compared with the minor groove width profiles extracted from NCP structures crystallized with sequence 601 (Figure 9, Table 4). In this approach, BII$_{i,j\ ext}$% is used as a suitable reporter of the groove shape of free DNA.

In the 5′ part and around the center of sequence 601, most wide or narrow minor grooves in the NCP X-ray structures correspond to peaks of intrinsic high and low BII propensities in free DNA, respectively. The quality of the match is particularly remarkable in the region covering SHL ± 2.5 (Figure 9, Table 4). On the 3′-side of sequence 601, the NCP groove widths at +2.5 helix turns or more from the NCP dyad are clearly out of phase with the corresponding free DNA BII propensities (Figure 9, Table 4). That is not inconsistent with the affinity data, as discussed below.

Table 4. Correlation Coefficients between the Minor Groove Width of DNA in NCP X-ray Structures and Intrinsic Extended BII Propensities[a]

sequence	affinity	whole seq	5′-end	central part	3′-end
		High Affinity Sequences			
f2	>601	0.51	0.65	0.73	−0.08
601L	>601	0.42	0.30	0.69	0.30
601	-	0.14	0.25	0.48	−0.63
618	<601	0.10	0.10	0.50	−0.03
		Low Affinity Sequences			
h2	≪601	0.07	0.18	0.11	−0.05
h3	≪601	0.16	0.14	0.28	0.12

[a]The minor groove width values were extracted from the NCP X-ray structures containing sequence 601 (PDB entries 3LZ0, 3LZ1, and 3MDV). The intrinsic extended BII propensities, BII$_{i,j\ ext}$% values defined in the text and Materials and Methods, were calculated along artificial sequences displaying either high (601, f2, 601L, 618) or low (h2, h3) affinity for the histone core. The affinities are ranked qualitatively with reference to sequence 601. The correlation coefficients calculated between BII$_{i,j\ ext}$% and minor groove width values were calculated on the whole sequences (SHL ± 7), or only for the 5′-end (SHL+2.5/SHL+7), or the central part (SHL ± 2.5), or the 3′end (SHL+2.5/SHL+7).

This analysis suggests that a part of the free sequence 601, in particular, its center, is predisposed to adopt an alternation of wide and narrow minor grooves favorable to NCP formation. To further investigate this idea, five artificial DNA sequences (Table 3) of various affinities (Table 4) for the histone core were examined. Sequence f2 is derived from sequence 601 by an enrichment in TpA steps and mutations in its 5′-part (http://genie.weizmann.ac.il/pubs/nucleosomes06/segal06_data.html). Sequence 601L is the palindromic derivative of the 5′ half of the sequence 601.[28] Both f2 and 601L displayed an affinity above that of their parent 601. Sequence 618 has a slightly lower affinity than sequence 601,[20] but still a good affinity for NCP formation. In contrast, sequences h2 and h3 have a very low ability to form nucleosomes (http://genie.weizmann.ac.il/pubs/nucleosomes06/segal06_data.html).

Free sequences 601, f2, 601L, and 618 have in common an alternation of minor groove widths in the NCPs, consonant with the variations of intrinsic BII$_{i,j\ ext}$% in the region covering

Table 3. Nucleosomal Sequences[a]

Sequence 618	CTGGCGCCTTTTCAAAGTTGTACCTGACCGAGCAGGTGCCTACAGATCCAGACGAGCGGAAATGCCCAGAATTGCGTCTACA-GACCGCTAAGCTCATCTAGAGCTCCCTAGAGCCACCAAGGGCTGTTCCCAGAAATTGTCGTAGAA
Sequence 601L	ATCACAATCCCGGTGCCGAGGCCGCTCAATTGGTCGTAGACAGCTCTAGCACCGCTTAAACGCACGTACGGAATCCGTACGTGC-GTTTAAGCGGTGCTAGAGCTGTCTACGACCAATTGAGCGGCCTCGGCACCGGGATTGTGAT
Sequence f2	CTGGAGATACCCGGTGCTAAGGCCGCTTAATTGGTCGTAGCAAGCTCTAGCACCGCTTAAACGCACGTACGCGCTGTCTACCGC-GTTTTAACCGCCAATAGGATTACTTACTAGTCTCTAGGCACGTGTAAGATATATACATCCTGT
Sequence h2	CTGGAGAATCCCGGTGCCGAGGCCGCTCAATGGATCCTAGCAAGCTCTAGGTGCGCTTAAACGGCTGTAGACGCCCTATCCTGTA-CGGCAGTTTAAGCGCACCTAGAGCCTCCGGAATTCACCACGTGTCAGATATATACATCCTGT
Sequence h3	CTGGAGAATCCCGGTGCCGAGGCCGCTCAATGGATCCTAGCATACTCTAGGTTAGCTTAAACTACTGTAGACTTACTGTACGGCAG-TTTAAGCTAACCTAGAGTACCCTCTCCGGAATTCACCACGTGTCAGATATATACATCCTGT

[a]Five artificial DNA sequences were selected to investigate to what extent their intrinsic properties relate to their affinities for the histone core: sequence 618,[20] sequence 601L,[28] and sequences f2, h2, and h3 (http://genie.weizmann.ac.il/pubs/nucleosomes06/segal06_data.html).

dx.doi.org/10.1021/bi500504y | Biochemistry 2014, 53, 5601−5612

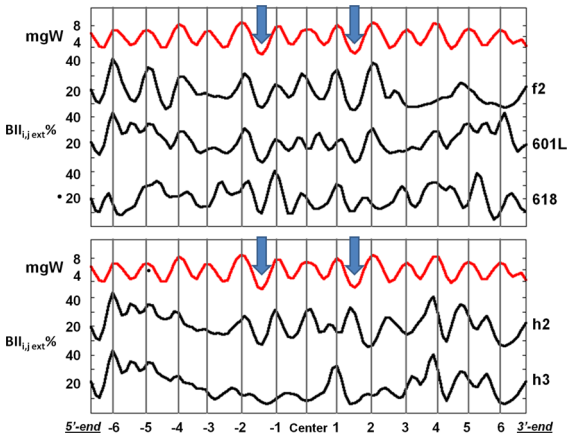

Figure 10. Intrinsic extended BII propensities of selected sequences, compared to variation of the minor groove width in the NCP X-ray structures. The sinusoidal variation of the minor groove width (mgW, Å) in the NCP structures is shown at the top of the panels (red line). The intrinsic backbone behavior is expressed in terms of BII$_{i,j\ ext}$% (see the text and Materials and Methods); variation along the sequences is traced with black lines (after smoothing with a spline approximation to the bars as shown in Figure 9). The vertical gray lines mark the maximal values of minor groove width, expressed in terms of SHL. The blue arrows indicate the location of SHL ± 1.5. The minor groove shape variations in the NCPs mainly follow the intrinsic extended BII propensities with sequences f2, 601L, and 618, but not sequences h2 and h3. That is consistent with sequences f2, 601L, and 618 being favorable to the NCP formation, while sequences h2 and h3 have a low affinity for the histone core.

SHL ± 2.5 (Figure 10, Table 4). Compared to sequence 601, this match extends on the 5′ side with f2 (Figure 10, Table 4). 601L, by duplicating the 5′ part of 601, improves the correlation along the 3′-side (Figure 10, Table 4). In contrast with these sequences best at forming NCP, the parallel between intrinsic BII$_{i,j\ ext}$% and minor groove width in NCPs is considerably weakened with both h2 and h3 (Figure 10, Table 4). A prominent discrepancy concerns SHL+1.5, which is composed of intrinsic BII-rich steps in h2 instead of intrinsic BI-rich steps in high affinity sequences (Figure 10). In h3, SHL+1.5 is composed of intrinsic BI steps, but a marked deficit of intrinsic BII steps characterizes its 3′ neighboring segment (Figure 10).

The pictorial analysis presented in Figure 10 was quantified by the regression correlation coefficients between intrinsic BII$_{i,j\ ext}$% and minor groove width in NCP. For the six considered sequences, the correlation coefficients parallel their affinities for the histone core (Table 4). This strongly supports the notion that the sequence-dependent intrinsic BII propensity of the nucleosomal sequences plays a role in NCP formation via its coupling with minor groove dimension in free DNAs. This explains why the palindromic derivative of the 5′ half of the 601 sequence (601L) displays a better affinity than its parent 601, and why the affinity of the palindromic derivative of the 3′ half is strongly reduced.[28] Also, the recurrence of a maximal agreement in the region SHL ± 2.5 (central 70 bp) in high affinity sequences would account for the remarkable conservation of this region in artificial DNAs selected for their maximal ability to form nucleosomes.[20]

The above results also support the importance of SHL ± 1.5 sequences. The SHL ± 1.5 regions in sequences 601, 601L, and f2 correspond to two TTAAA fragments. According to the three nucleosome structures crystallized with sequence 601,[26,27] TTAAA segments robustly anchor histones H3 and H4 owing to hydrophobic interactions and an electrostatic interaction between Arg63 of H3 and the TTAAA minor groove.[5,28] The bound TTAAA segments are characterized by sustained narrow minor grooves (3−4 Å) and variable negative rolls (ApA•TpT: −6.2 ± 5.8°; TpA•TpA: −8.9 ± 8.8°) associated with the curvature. On the trinucleotide fragment TAA•TTA, these negative rolls are associated with BI•BII facing phosphate linkages, following the intrinsic trend in free DNA.[34,38,40,41]

The present NMR data show that the whole free TTAAA element is composed of BI-rich steps (Figure 7) associated with a narrow minor groove (Scheme 1). BI-rich TpA and ApA•TpT dinucleotides intrinsically favor null or positive rolls.[38,64] The structures of oligomers containing T_nA_n crystallized in various space groups corroborate the presence of positive rolls in such sequences.[65] So, free and bound TTAAA elements share the narrowing of the minor groove but not the rolls. The deformation of intrinsic null or positive rolls toward negative rolls in the NCPs may have an energetic cost. This cost may be compensated by the negative electrostatic potential generated by the DNA minor grooves, which is especially enhanced in the case of narrow A•T-rich minor grooves.[66] Such strong electronegative potential associated with the pre-existing narrow minor groove of TTAAA segments could drive the recognition of Arg63 of H3, initializing the anchoring of histones and counterbalancing the cost incurred by negative rolls.

The SHL ± 1.5 elements are surrounded by G•C rich sequences (in sequence 601: CCGCTTAAACGCA in SHL-1.5 and GCGTTTTAACCGC in SHL+1.5) that, in the NCP, adopt the widest minor grooves of ∼8 Å (Figures 9 and 10). This is also consistent with the intrinsic structural preferences of free DNA. The flanking regions of SHL-1.5 and SHL+1.5 are composed of dinucleotides with BII as stable as, or even more stable than, BI (Table 2 and Figure 7). Such BII-rich regions in free DNA explore a large conformational landscape that produces minor grooves on average clearly wider than BI-rich segments, as shown in this work. The presence of two or more phosphate linkages simultaneously in BII within a tetrameric segment is in fact associated with minor groove widths reaching 7−8 Å,[47] as large as those observed in the NCPs.

In sum, both TTAAA elements and their flanking regions have intrinsic minor groove properties that are favorable to nucleosome formation. A key point concerns the two TTAAA motifs, symmetrically located around the nucleosome dyad (SHL ± 1.5) and distant by 30 bp, which allow the anchoring of the two Arg63 of H3 dimer in their narrow, negatively charged, minor groove. Such minor groove intrinsic characteristics are retrieved on another A•T-rich element, GATTA at SHL+3 (Figure 9), which could thus also accommodate one arginine. However, these favorable intrinsic properties are lost in the corresponding 30 bp upstream region, CGCTG at SHL 0, predicted to adopt a wide minor groove with a weakened negative potential. Within the whole sequence 601, TTAAA elements at SHL ± 1.5 emerge as a unique, attractive combination to capture the two Arg63 of H3 dimer.

Taken together, the above results strongly suggest that the sequence-dependent intrinsic structural properties of free DNA contribute to the particularly strong affinity of the sequence 601 and its derivatives for the histone core. They are consistent with a crucial role of pre-existing structural preferences for a regular alternation of wide and narrow minor grooves for NCP indirect readout.

dx.doi.org/10.1021/bi500504y | *Biochemistry* 2014, 53, 5601−5612

CONCLUSION

Using NMR, we studied four DNA dodecamers relevant to a better understanding of the formation of nucleosome core particles (NCPs). When juxtaposed (discarding the terminal base pairs) these dodecamers recompose a 39 bp fragment of the 5′ part of the sequence 601 of very high affinity for the histone core.[20] To investigate how DNA intrinsic properties affect the ability to form nucleosomes, one exploited the BI ↔ BII equilibrium of the phosphate groups, which is convenient and reliable reporter of the behavior of dinucleotides in B-DNA.[34,38,47] The results provide convincing evidence that the sequence-dependent minor groove shape influences the indirect readout mechanism underlying the nucleosome formation.

The studied dodecamers contain dinucleotides with BI-rich (high-field shifted δPs) or BII-rich (downfield shifted δPs) phosphate linkages. The examination of δP changes in function of temperature provided additional support of the reliability of the methods used to derive BII populations from δPs.[38,39] Importantly, the newly collected δPs enabled us to validate the sequence dependence of the BII propensities. It confirmed that it is dominated by the dinucleotide sequence and therefore is predictable, as previously proposed.[34] From a structural point of view, the NMR data validate the proposition based on X-ray structure analyses[47] that the phosphate groups inform on the minor groove width. As a result, high and low BII densities in DNA tetramer segments free in solution are coupled to wide and narrow minor grooves, respectively.

Taken together, these results offer a specific and powerful framework to address the role of minor groove shape in the nucleosome formation process. The prediction of intrinsic BII propensities was applied to several sequences with various abilities at forming nucleosomes. This approach does not mean that the histone core directly recognizes the backbone states themselves, nor does it suggest that the BII locations should be similar in free and nucleosomal DNAs. Indeed, the backbone angles behave differently in free and bound DNAs, with in particular the emergence of numerous α/γ conformers typical of bound DNAs.[40,67,68] In our approach, the intrinsic BII propensities are considered reporters of helicoidal features, in particular, the minor groove width.

Only sequences of high affinity for the histone core were found to exhibit intrinsic BII density profiles—representative of minor groove width profiles—that largely parallel the recurrent, characteristic variations of minor groove width in NCP X-ray structures (Figures 9 and 10). The maximal agreement observed along the central ∼70 bp is particularly interesting because this region is contacted at the first stage of the nucleosome formation[23,24] and highly conserved in the highest-affinity artificial sequences.[20] Our results also provide new insights on the lexicographic periodicity of ∼10 bp found in nucleosomal positioning sequences, *in vitro* and *in vivo*. Such positioning sequences consist of regions enriched in CpG•CpG, GpC•GpC, CpA•TpG, and GpC•CpC that alternate with ApA•TpT, TpA•TpA, and ApT•ApT rich segments.[9−18] According to our analysis, the first group of dinucleotides imparts free DNA segments with high BII density associated with wide minor grooves; the second group forms BI-rich regions with intrinsic narrow minor grooves. The alternation of both groups seems essential since sequences containing numerous A_n•T_n tracts, unable to spontaneously generate wide minor groove, disfavor nucleosome deposition.[69,70] Finally, our findings are consistent with a study reporting that the narrowest minor grooves in free yeast sequences known to be occupied by nucleosomes *in vivo* are compatible with their counterparts in NCP DNA.[71] Hence, the minor groove width in free B-DNA appears as a key structural determinant in the indirect readout process underlying the NCP formation.

Indirect readout exploiting variations of minor groove shape was also demonstrated on the DNA−DNase I interaction.[50] This enzyme interacts with any DNA minor groove but preferentially cuts sequences adjacent to BII-rich regions, because widening of the minor groove favors the binding of DNase I.[50] Also, the architectural bacterial protein Fis binds DNA with no obvious sequence selectivity but prefers A•T-rich regions with intrinsic narrow minor groove; three or more A•T → G•C base pair substitutions severely decrease Fis binding by altering the minor groove shape.[72] The concept of groove shape indirect readout was generalized based on an analysis of exhaustive sets of X-ray structures.[30,47] Thus, the crucial role of preformed grooves in DNA nucleosomal positioning sequences is not an isolated case. The ability to predict the DNA minor groove shape directly from its sequence not only provides a basis to interpret the effect of mutations on nucleosome formation, but also may help to uncover more examples where this shape is critical to DNA recognition.

In vitro nucleosome binding experiments showed that the temperature affects the nucleosome formation and suggested a role of entropy in this process.[73] Also, ions can potentially influence nucleosome positioning.[2,74] The observations that temperature (this study and [39,58]) and cations[64,75] modulate the phosphate group behavior and consequently the DNA shape are very interesting in this context, although more work is needed to determine the extent to which these factors might influence the nucleosome formation.

The nucleosome organization *in vivo* is likely determined through an interplay between intrinsic DNA properties, chromatin remodelers, and competition with nonhistone proteins bound to DNA.[76] The relative importance of these factors contributing to the positioning remains controversial. Yet, recent studies confirm that DNA sequence does play a role in positioning nucleosomes *in vivo*, by influencing nucleosome assembly, stability, and disassembly.[10,76−78] Extensive mappings of nucleosome positioning highlight the heterogeneity of such positioning, with regions of precise and high nucleosome occupancy and other regions where the positioning is much more diffuse.[79−81] The approach described in the present work could help interpret the large data from such mappings, especially since the proposed sequence-based approach lends itself to high-throughput computational processing.

ASSOCIATED CONTENT

Supporting Information

Tables S1 and S2: ^{31}P chemical shifts determined in this study. Figure S1: Variations of internucleotides distances depending on BII percentages. Figure S2: Sequence effect on BII propensities for complementary dinucleotides present in several copies in the studied dodecamers. Figure S3: Sequence effect on extended BII propensities of the complementary dinucleotides of the four dodecamers. This material is available free of charge via the Internet at http://pubs.acs.org.

AUTHOR INFORMATION

Corresponding Authors

*E-mail: olivier.mauffret@lbpa.ens-cachan.fr. Tel.: +33-147407421. Fax: +33-147407671.

*E-mail: bhartman@ens-cachan.fr. Tel.: +33-147407421. Fax: +33-147407671.

Author Contributions

Xiaoqian Xu and Akli Ben Imeddourene have equally contributed to the work. Akli Ben Imeddourene and Xiaoqian Xu performed the NMR experiments under the supervision of Loussiné Zargarian and Olivier Mauffret. Akli Ben Imeddourene carried out most analyses. Brigitte Hartmann, the project leader, wrote the manuscript with Nicolas Foloppe.

Notes

The authors declare no competing financial interest.

■ ACKNOWLEDGMENTS

The East China Normal University is gratefully acknowledged for its support. The authors thank Drs Sylvie Rimsky (LBPA, CNRS/ENS de Cachan) and Christophe Oguey (LPTM, Université de Cergy-Pontoise) for helpful advice.

■ REFERENCES

(1) Andrews, A. J., and Luger, K. (2011) Nucleosome structure(s) and stability: variations on a theme. *Annu. Rev. Biophys 40*, 99−117.
(2) Davey, C. A., Sargent, D. F., Luger, K., Maeder, A. W., and Richmond, T. J. (2002) Solvent mediated interactions in the structure of the nucleosome core particle at 1.9 a resolution. *J. Mol. Biol. 319*, 1097−1113.
(3) Luger, K., Mader, A. W., Richmond, R. K., Sargent, D. F., and Richmond, T. J. (1997) Crystal structure of the nucleosome core particle at 2.8 A resolution. *Nature 389*, 251−260.
(4) Olson, W. K., and Zhurkin, V. B. (2011) Working the kinks out of nucleosomal DNA. *Curr. Opin. Struct. Biol. 21*, 348−357.
(5) Wu, B., Mohideen, K., Vasudevan, D., and Davey, C. A. (2010) Structural insight into the sequence dependence of nucleosome positioning. *Structure 18*, 528−536.
(6) Xu, F., and Olson, W. K. (2010) DNA architecture, deformability, and nucleosome positioning. *J. Biomol. Struct. Dyn. 27*, 725−739.
(7) Balasubramanian, S., Xu, F., and Olson, W. K. (2009) DNA sequence-directed organization of chromatin: structure-based computational analysis of nucleosome-binding sequences. *Biophys. J. 96*, 2245−2260.
(8) Richmond, T. J., and Davey, C. A. (2003) The structure of DNA in the nucleosome core. *Nature 423*, 145−150.
(9) Widom, J. (2001) Role of DNA sequence in nucleosome stability and dynamics. *Q. Rev. Biophys. 34*, 269−324.
(10) Brogaard, K., Xi, L., Wang, J. P., and Widom, J. (2012) A map of nucleosome positions in yeast at base-pair resolution. *Nature 486*, 496−501.
(11) Cui, F., and Zhurkin, V. B. (2010) Structure-based analysis of DNA sequence patterns guiding nucleosome positioning in vitro. *J. Biomol. Struct. Dyn. 27*, 821−841.
(12) Drew, H. R., and Calladine, C. R. (1987) Sequence-specific positioning of core histones on an 860 base-pair DNA. Experiment and theory. *J. Mol. Biol. 195*, 143−173.
(13) Drew, H. R., and Travers, A. A. (1985) DNA bending and its relation to nucleosome positioning. *J. Mol. Biol. 186*, 773−790.
(14) Kaplan, N., Moore, I. K., Fondufe-Mittendorf, Y., Gossett, A. J., Tillo, D., Field, Y., LeProust, E. M., Hughes, T. R., Lieb, J. D., Widom, J., and Segal, E. (2009) The DNA-encoded nucleosome organization of a eukaryotic genome. *Nature 458*, 362−366.
(15) Satchwell, S. C., Drew, H. R., and Travers, A. A. (1986) Sequence periodicities in chicken nucleosome core DNA. *J. Mol. Biol. 191*, 659−675.
(16) Segal, E., Fondufe-Mittendorf, Y., Chen, L., Thastrom, A., Field, Y., Moore, I. K., Wang, J. P., and Widom, J. (2006) A genomic code for nucleosome positioning. *Nature 442*, 772−778.
(17) Takasuka, T. E., and Stein, A. (2010) Direct measurements of the nucleosome-forming preferences of periodic DNA motifs challenge established models. *Nucleic Acids Res. 38*, 5672−5680.
(18) Travers, A., Hiriart, E., Churcher, M., Caserta, M., and Di Mauro, E. (2010) The DNA sequence-dependence of nucleosome positioning in vivo and in vitro. *J. Biomol. Struct. Dyn. 27*, 713−724.
(19) Olson, W. K., Gorin, A. A., Lu, X. J., Hock, L. M., and Zhurkin, V. B. (1998) DNA sequence-dependent deformability deduced from protein-DNA crystal complexes. *Proc. Natl. Acad. Sci. U.S.A. 95*, 11163−11168.
(20) Thastrom, A., Bingham, L. M., and Widom, J. (2004) Nucleosomal locations of dominant DNA sequence motifs for histone-DNA interactions and nucleosome positioning. *J. Mol. Biol. 338*, 695−709.
(21) Miele, V., Vaillant, C., d'Aubenton-Carafa, Y., Thermes, C., and Grange, T. (2008) DNA physical properties determine nucleosome occupancy from yeast to fly. *Nucleic Acids Res. 36*, 3746−3756.
(22) Hall, M. A., Shundrovsky, A., Bai, L., Fulbright, R. M., Lis, J. T., and Wang, M. D. (2009) High-resolution dynamic mapping of histone-DNA interactions in a nucleosome. *Nat. Struct. Mol. Biol. 16*, 124−129.
(23) Cremisi, C., and Yaniv, M. (1980) Sequential assembly of newly synthesized histones on replicating SV40 DNA. *Biochem. Biophys. Res. Commun. 92*, 1117−1123.
(24) Worcel, A., Han, S., and Wong, M. L. (1978) Assembly of newly replicated chromatin. *Cell 15*, 969−977.
(25) Fernandez, A. G., and Anderson, J. N. (2007) Nucleosome positioning determinants. *J. Mol. Biol. 371*, 649−668.
(26) Makde, R. D., England, J. R., Yennawar, H. P., and Tan, S. (2010) Structure of RCC1 chromatin factor bound to the nucleosome core particle. *Nature 467*, 562−566.
(27) Vasudevan, D., Chua, E. Y., and Davey, C. A. (2010) Crystal structures of nucleosome core particles containing the '601' strong positioning sequence. *J. Mol. Biol. 403*, 1−10.
(28) Chua, E. Y., Vasudevan, D., Davey, G. E., Wu, B., and Davey, C. A. (2012) The mechanics behind DNA sequence-dependent properties of the nucleosome. *Nucleic Acids Res. 40*, 6338−6352.
(29) Ong, M. S., Richmond, T. J., and Davey, C. A. (2007) DNA stretching and extreme kinking in the nucleosome core. *J. Mol. Biol. 368*, 1067−1074.
(30) Rohs, R., Jin, X., West, S. M., Joshi, R., Honig, B., and Mann, R. S. (2010) Origins of specificity in protein-DNA recognition. *Annu. Rev. Biochem. 79*, 233−269.
(31) West, S. M., Rohs, R., Mann, R. S., and Honig, B. (2010) Electrostatic interactions between arginines and the minor groove in the nucleosome. *J. Biomol. Struct. Dyn. 27*, 861−866.
(32) Foloppe, N., Gueroult, M., and Hartmann, B. (2013) Simulating DNA by molecular dynamics: aims, methods, and validation. *Methods Mol. Biol. 924*, 445−468.
(33) Heddi, B., Foloppe, N., Oguey, C., and Hartmann, B. (2008) Importance of accurate DNA structures in solution: the Jun-Fos model. *J. Mol. Biol. 382*, 956−970.
(34) Heddi, B., Oguey, C., Lavelle, C., Foloppe, N., and Hartmann, B. (2010) Intrinsic flexibility of B-DNA: the experimental TRX scale. *Nucleic Acids Res. 38*, 1034−1047.
(35) Fratini, A. V., Kopka, M. L., Drew, H. R., and Dickerson, R. E. (1982) Reversible bending and helix geometry in a B-DNA dodecamer: CGCGAATTBrCGCG. *J. Biol. Chem. 257*, 14686−14707.
(36) Gorenstein, D. G. (1984) *Phosphorus-31 NMR: Principles and Applications*, Academic Press, New York.
(37) Gorenstein, D. G. (1992) ^{31}P NMR of DNA. *Methods Enzymol. 211*, 254−286.
(38) Heddi, B., Foloppe, N., Bouchemal, N., Hantz, E., and Hartmann, B. (2006) Quantification of DNA BI/BII backbone states in solution. Implications for DNA overall structure and recognition. *J. Am. Chem. Soc. 128*, 9170−9177.
(39) Tian, Y., Kayatta, M., Shultis, K., Gonzalez, A., Mueller, L. J., and Hatcher, M. E. (2009) ^{31}P NMR investigation of backbone dynamics in DNA binding sites†. *J. Phys. Chem. B 113*, 2596−2603.

(40) Djuranovic, D., and Hartmann, B. (2003) Conformational characteristics and correlations in crystal structures of nucleic acid oligonucleotides: evidence for sub-states. *J. Biomol. Struct. Dyn. 20*, 771−788.
(41) Djuranovic, D., and Hartmann, B. (2004) DNA fine structure and dynamics in crystals and in solution: the impact of BI/BII backbone conformations. *Biopolymers 73*, 356−368.
(42) Hartmann, B., Piazzola, D., and Lavery, R. (1993) BI-BII transitions in B-DNA. *Nucleic Acids Res. 21*, 561−568.
(43) Srinivasan, A. R., and Olson, W. K. (1987) Nucleic acid model building: the multiple backbone solutions associated with a given base morphology. *J. Biomol. Struct. Dyn. 4*, 895−938.
(44) van Dam, L., and Levitt, M. H. (2000) BII nucleotides in the B and C forms of natural-sequence polymeric DNA: A new model for the C form of DNA. *J. Mol. Biol. 304*, 541−561.
(45) Winger, R. H., Liedl, K. R., Pichler, A., Hallbrucker, A., and Mayer, E. (1999) Helix morphology changes in B-DNA induced by spontaneous B(I)≤=>B(II) substrate interconversion. *J. Biomol. Struct. Dyn. 17*, 223−235.
(46) Drsata, T., Perez, A., Orozco, M., Morozov, A. V., Sponer, J., and Lankas, F. (2013) Structure, stiffness and substates of the dickerson-drew dodecamer. *J. Chem. Theory Comput. 9*, 707−721.
(47) Oguey, C., Foloppe, N., and Hartmann, B. (2010) Understanding the sequence-dependence of DNA groove dimensions: implications for DNA interactions. *PLoS One 5*, e15931.
(48) Prive, G. G., Yanagi, K., and Dickerson, R. E. (1991) Structure of the B-DNA decamer C-C-A-A-C-G-T-T-G-G and comparison with isomorphous decamers C-C-A-A-G-A-T-T-G-G and C-C-A-G-G-C-C-T-G-G. *J. Mol. Biol. 217*, 177−199.
(49) Wang, D., Ulyanov, N. B., and Zhurkin, V. B. (2010) Sequence-dependent Kink-and-Slide deformations of nucleosomal DNA facilitated by histone arginines bound in the minor groove. *J. Biomol. Struct. Dyn. 27*, 843−859.
(50) Heddi, B., Abi-Ghanem, J., Lavigne, M., and Hartmann, B. (2010) Sequence-dependent DNA flexibility mediates DNase I cleavage. *J. Mol. Biol. 395*, 123−133.
(51) Delaglio, F., Grzesiek, S., Vuister, G. W., Zhu, G., Pfeifer, J., and Bax, A. (1995) NMRPipe: a multidimensional spectral processing system based on UNIX pipes. *J. Biomol. NMR 6*, 277−293.
(52) Piotto, M., Saudek, V., and Sklenar, V. (1992) Gradient-tailored excitation for single-quantum NMR spectroscopy of aqueous solutions. *J. Biomol. NMR 2*, 661−665.
(53) Baleja, J. D., Moult, J., and Sykes, B. D. (1990) Distance measurement and structure refinement with Noe data. *J. Magn. Reson. 87*, 375−384.
(54) Sklenar, V., Miyashiro, H., Zon, G., Miles, H. T., and Bax, A. (1986) Assignment of the 31P and 1H resonances in oligonucleotides by two-dimensional NMR spectroscopy. *FEBS Lett. 208*, 94−98.
(55) Lavery, R., Moakher, M., Maddocks, J. H., Petkeviciute, D., and Zakrzewska, K. (2009) Conformational analysis of nucleic acids revisited: Curves+. *Nucleic Acids Res. 37*, 5917−5929.
(56) Precechtelova, J., Munzarova, M. L., Vaara, J., Novotny, J., Dracinski, M., and Sklenar, V. (2013) Toward reproducing sequence trends in phosphorus chemical shifts for nucleic acids by MD/DFT calculations. *J. Chem. Theory Comput. 9*, 1641−1656.
(57) Ho, C. N., and Lam, S. L. (2004) Random coil phosphorus chemical shift of deoxyribonucleic acids. *J. Magn. Reson. 171*, 193−200.
(58) Nikonowicz, E. P., and Gorenstein, D. G. (1990) Two-dimensional 1H and 31P NMR spectra and restrained molecular dynamics structure of a mismatched GA decamer oligodeoxyribonucleotide duplex. *Biochemistry 29*, 8845−8858.
(59) Nikolova, E. N., Kim, E., Wise, A. A., O'Brien, P. J., Andricioaei, I., and Al-Hashimi, H. M. (2011) Transient Hoogsteen base pairs in canonical duplex DNA. *Nature 470*, 498−502.
(60) Lefebvre, A., Mauffret, O., Hartmann, B., Lescot, E., and Fermandjian, S. (1995) Structural behavior of the CpG step in two related oligonucleotides reflects its malleability in solution. *Biochemistry 34*, 12019−12028.
(61) Tisne, C., Delepierre, M., and Hartmann, B. (1999) How NF-kappaB can be attracted by its cognate DNA. *J. Mol. Biol. 293*, 139−150.
(62) Stofer, E., and Lavery, R. (1994) Measuring the geometry of DNA grooves. *Biopolymers 34*, 337−346.
(63) Chuprina, V. P., Lipanov, A. A., Fedoroff, O., Kim, S. G., Kintanar, A., and Reid, B. R. (1991) Sequence effects on local DNA topology. *Proc. Natl. Acad. Sci. U.S.A. 88*, 9087−9091.
(64) Heddi, B., Foloppe, N., Hantz, E., and Hartmann, B. (2007) The DNA structure responds differently to physiological concentrations of K(+) or Na(+). *J. Mol. Biol. 368*, 1403−1411.
(65) Mack, D. R., Chiu, T. K., and Dickerson, R. E. (2001) Intrinsic bending and deformability at the T-A step of CCTTTAAAGG: a comparative analysis of T-A and A-T steps within A-tracts. *J. Mol. Biol. 312*, 1037−1049.
(66) Rohs, R., West, S. M., Sosinsky, A., Liu, P., Mann, R. S., and Honig, B. (2009) The role of DNA shape in protein-DNA recognition. *Nature 461*, 1248−1253.
(67) Djuranovic, D., and Hartmann, B. (2005) Molecular dynamics studies on free and bound targets of the bovine papillomavirus type I e2 protein: the protein binding effect on DNA and the recognition mechanism. *Biophys. J. 89*, 2542−2551.
(68) Varnai, P., Djuranovic, D., Lavery, R., and Hartmann, B. (2002) Alpha/gamma transitions in the B-DNA backbone. *Nucleic Acids Res. 30*, 5398−5406.
(69) Hughes, A., and Rando, O. J. (2009) Chromatin 'programming' by sequence–is there more to the nucleosome code than %GC? *J. Biol. 8*, 96.
(70) Segal, E., and Widom, J. (2009) Poly(dA:dT) tracts: major determinants of nucleosome organization. *Curr. Opin. Struct. Biol. 19*, 65−71.
(71) Bishop, E. P., Rohs, R., Parker, S. C., West, S. M., Liu, P., Mann, R. S., Honig, B., and Tullius, T. D. (2011) A map of minor groove shape and electrostatic potential from hydroxyl radical cleavage patterns of DNA. *ACS Chem. Biol. 6*, 1314−1320.
(72) Stella, S., Cascio, D., and Johnson, R. C. (2010) The shape of the DNA minor groove directs binding by the DNA-bending protein Fis. *Genes Dev. 24*, 814−826.
(73) Wu, C., and Travers, A. (2005) Relative affinities of DNA sequences for the histone octamer depend strongly upon both the temperature and octamer concentration. *Biochemistry 44*, 14329−14334.
(74) Davey, C. A., and Richmond, T. J. (2002) DNA-dependent divalent cation binding in the nucleosome core particle. *Proc. Natl. Acad. Sci. U.S.A. 99*, 11169−11174.
(75) Gueroult, M., Boittin, O., Mauffret, O., Etchebest, C., and Hartmann, B. (2012) Mg2+ in the major groove modulates B-DNA structure and dynamics. *PLoS One 7*, e41704.
(76) Struhl, K., and Segal, E. (2013) Determinants of nucleosome positioning. *Nat. Struct. Mol. Biol. 20*, 267−273.
(77) Parmar, J. J., Marko, J. F., and Padinhateeri, R. (2014) Nucleosome positioning and kinetics near transcription-start-site barriers are controlled by interplay between active remodeling and DNA sequence. *Nucleic Acids Res. 42*, 128−136.
(78) Raveh-Sadka, T., Levo, M., Shabi, U., Shany, B., Keren, L., Lotan-Pompan, M., Zeevi, D., Sharon, E., Weinberger, A., and Segal, E. (2012) Manipulating nucleosome disfavoring sequences allows fine-tune regulation of gene expression in yeast. *Nat. Genetics 44*, 743−750.
(79) Jansen, A., and Verstrepen, K. J. (2011) Nucleosome positioning in Saccharomyces cerevisiae. *Microbiol. Mol. Biol. Rev. 75*, 301−320.
(80) Korber, P. (2012) Active nucleosome positioning beyond intrinsic biophysics is revealed by in vitro reconstitution. *Biochem. Soc. Trans. 40*, 377−382.
(81) Zhang, Z., and Pugh, B. F. (2011) High-resolution genome-wide mapping of the primary structure of chromatin. *Cell 144*, 175−186.